Journal of The Electrochemical Society, **152** (1) A132-A140 (2005)
0013-4651/2004/152(1)/A132/9/$7.00 © The Electrochemical Society, Inc.

Conductivity and Viscosity of PC-DEC and PC-EC Solutions of LiBOB

Michael S. Ding,*,z Kang Xu,* and T. Richard Jow*

Army Research Laboratory, Adelphi, Maryland 20783, USA

Conductivity κ of propylene carbonate-diethyl carbonate (PC-DEC) and propylene carbonate-ethylene carbonate (PC-EC) solutions of lithium bis(oxalato)borate (LiBOB) was experimentally determined at temperatures θ from 60 to −80°C, salt molalities m from 0.04 to 1.1 mol kg^{-1}, and solvent compositions w from 0 to 0.7 weight fraction of DEC and EC. Viscosity η of LiBOB in PC-EC was studied through measuring its glass transition temperature T_g in the same ranges of m and w. T_g was found to rise with m and w of EC, indicating a concurrent change in the η of the solution. The κ of the PC-DEC solution of LiBOB peaked in both m and w thus forming a ''dome'' in its 3D presentation in the coordinates of m and w, while that of the PC-EC solution peaked only in m resulting in an ''arch''-shaped surface. As the θ was lowered, these κ surfaces fell in height and shifted in the direction of low η. These observations correlated well with the changes of dielectric constant of the solvents and η of the solutions with the same set of variables. The measured $\kappa(T)$ data for the PC-DEC solution was fitted with the Vogel-Tamman-Fulcher equation for an evaluation of its vanishing mobility temperature and apparent activation energy. The results of κ and η of the LiBOB solutions were further compared with those of $LiPF_6$ solutions from a previous study.
 [DOI: 10.1149/1.1833611]

Manuscript submitted March 17, 2004; revised manuscript received May 11, 2004. Available electronically December 1, 2004.

This report parallels two earlier ones[1,2] in both structure and content, those dealing with conductivities and viscosities of propylene carbonate-diethyl carbonate (PC-DEC) and propylene carobonate-ethylene carbonate (PC-EC) solutions of $LiPF_6$ and $LiBF_4$, respectively; this report dealing with lithium bis(oxalato)borate (LiBOB).[3] As such, this report, while giving full account of the new experimental results, skips over some of the detailed descriptions and explanations that can be found in previous reports. Also, although the measured properties of LiBOB are briefly compared with those of $LiPF_6$ in this report, a fuller comparison across all three salts and its discussion will be left to another report that is to follow.

The aim of this report is mainly to provide a relatively complete picture for the change of conductivity κ with salt molality m and solvent weight fraction w at different temperatures θ (θ symbolizes temperature in degrees centigrade and T in degrees of absolute temperature, K)[3] for PC-DEC and PC-EC solutions of LiBOB, denoted here as $(LiBOB)_m$-$PC_{1-w}DEC_w$ and $(LiBOB)_m$-$PC_{1-w}EC_w$. It is felt that such a picture, together with what is already known of dielectric constant ε and viscosity η of PC-DEC and PC-EC solvents and of κ and η of their electrolytes of $LiBF_4$ and $LiPF_6$,[1,2,4,5] could lead to a clear demonstration of the similarities and differences in the change of κ with m and w and with θ for the three important lithium salts in the carbonate solvents and to an elucidation of the mechanisms giving rise to these similarities and differences.

As has been amply demonstrated, κ of an electrolyte of a particular salt is critically dependent on the ε of the solvent and the η of the electrolyte:—κ rises with a high ε which promotes ion dissociation and with a low η which facilitates ion movement.[6-9] For this reason, ε and η of many solvents and κ and η of many electrolytes have been measured as functions of w, m, and θ in regard to their application to lithium-ion batteries.[1,4-17] In particular, in connection to this study, ε of PC-DEC and PC-EC solvents has been systematically measured and found to change monotonically and smoothly with w and θ. ε falls with θ universally, and falls with w in $PC_{1-w}DEC_w$ but rises in $PC_{1-w}EC_w$[4] (ε of DEC, PC, and EC at 40°C: 2.809, 61.43, and 89.78[12,18]), as has been similarly observed for many other related solvents.[8-10,13,19-21] Accordingly, Bjerrum critical distance for univalent ions has been calculated to be nearly independent of θ but strongly dependent on w, rising steadily as ε falls with the change of w, indicating a corresponding change in ion association.[4] The η of the solvents has been estimated by measuring their glass transition temperature T_g, and found to fall steadily with w in $PC_{1-w}DEC_w$ but rise in $PC_{1-w}EC_w$[4] (η of DEC, PC, and EC at 40°C: 0.622, 1.91, and 1.93 mPa s[12,18]), as would normally be expected between similar liquids.[4,6,8,9,11,13,19,22-24] Furthermore, the η of $(LiPF_6)_m$-$PC_{1-w}DEC_w$, $(LiPF_6)_m$-$PC_{1-w}EC_w$, $(LiBF_4)_m$-$PC_{1-w}DEC_w$, and $(LiBF_4)_m$-$PC_{1-w}EC_w$ solutions has been found to rise with m and fall with w of DEC but rise with w of EC.[1,2] κ has been found to peak in both m and w for $(LiPF_6)_m$-$PC_{1-w}DEC_w$ and $(LiBF_4)_m$-$PC_{1-w}DEC_w$ thus forming a dome in the mw-coordinates but only in m for $(LiPF_6)_m$-$PC_{1-w}EC_w$ and $(LiBF_4)_m$-$PC_{1-w}EC_w$ thus forming an arch.[1,2] As θ is lowered, these κ surfaces lower their heights and shift their positions in the direction of low η.[1,2,5] This series of investigation was continued with the work to be presented here, in which $(LiBOB)_m$-$PC_{1-w}DEC_w$ and $(LiBOB)_m$-$PC_{1-w}EC_w$ solutions were studied for their κ and η. The choice for these materials was a result of the strong interest in and the wide use of these three lithium salts

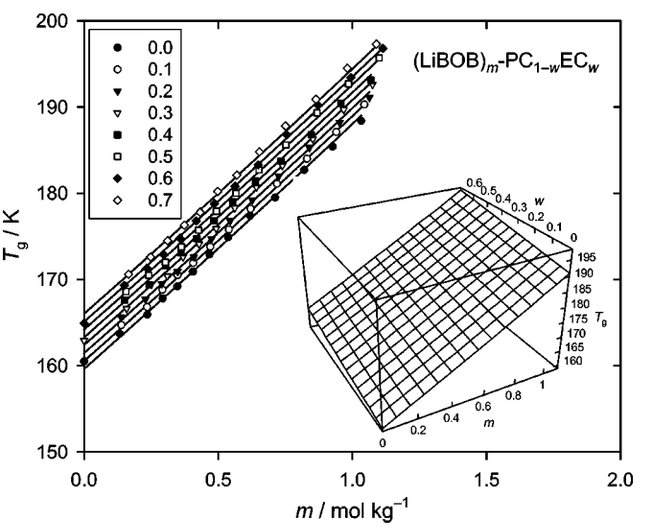

Figure 1. Change of glass transition temperature $T_g$with salt molality m and solvent weight fraction w for $(LiBOB)_m$-$PC_{1-w}EC_w$ solution. The symbols represent the measured data and the curves plot their fitting function of Eq. 1, which is also plotted as a 3D surface as inserted in the figure.

* Electrochemical Society Active Member.
z E-mail: mding@arl.army.mil

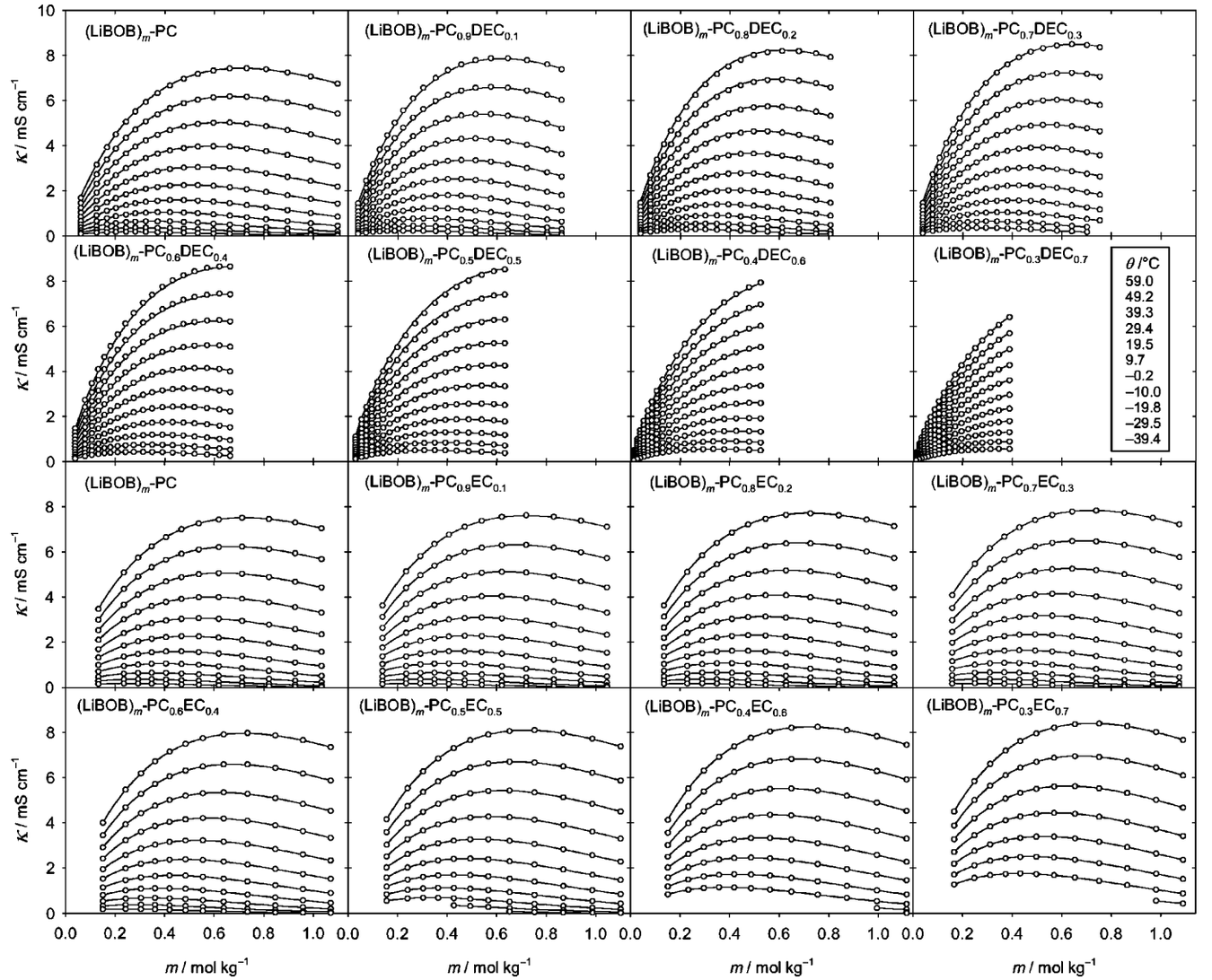

Figure 2. Change of conductivity κ with salt molality m at different temperatures θ and solvent weight fractions w for (LiBOB)$_m$-PC$_{1-w}$DEC$_w$ and (LiBOB)$_m$-PC$_{1-w}$EC$_w$ solutions. The open circles represent measured data and the curves plot their fitting functions. The absence of concentrated (LiBOB)$_m$-PC$_{1-w}$DEC$_w$ electrolytes with a high w was due to the limited solubility of LiBOB in these solvents.

and their carbonate electrolytes,[25-27] the great variation in ε and in the nature of the solvents, and the low melting points of PC and DEC and the strong resistance of PC to crystallization.[1,4,28]

Experimental

LiBOB was synthesized in our laboratory following an aqueous approach by Lischka *et al.*[29] and purified to above 99% by repeated recrystallizations.[30] PC of 99.98% purity and DEC and EC both of 99.95% were purchased from Grant Chemical and used without further treatment. Starting solutions with high concentrations of LiBOB in the various solvents of PC-DEC and PC-EC were prepared in an argon-filled dry box. Measurement of κ on these solutions and their subsequent dilution for the next set of less concentrated solutions were carried out in a dry room. At the end of each measurement, a small amount of sample was taken from each electrolyte, on which the T_g was determined with a modulated differential scanning calorimeter (MDSC 2920, TA Instruments) cooled with liquid nitrogen. The κ of the solutions was measured with an impedance scan from 1 MHz to 20 Hz obtained with an 4284A precision LCR meter at selected temperatures within a Tenney Jr. Environmental Chamber. The overall measurement error was estimated to be 0.5% in κ and 0.5 K in T_g. More experimental details on the determination of T_g and κ can be found elsewhere.[12,4-6]

Results and Discussion

Change of viscosity with salt content and solvent composition.—Figure 1 plots the results of measurement of T_g for (LiBOB)$_m$-PC$_{1-w}$EC$_w$ solution, with the symbols for the measured data and the curves for their fitting function

$$T_g = 159.62 + 27.483m + 0.92432m^2 + 9.1297w \qquad [1]$$

where T_g is in the unit of K, the application limits are 0 to 1.1 mol kg^{-1} for m and 0 to 0.7 weight fraction for w, and the fitting error is 0.86% of the data range. This equation is also plotted as a T_g surface in the mw-coordinates as the insert in the figure, describing a simple surface slanting down from the high-η corner of high m and w toward the low-η corner of low m and w. It is thus clear that the addition of LiBOB in PC$_{1-w}$EC$_w$ solvent continuously raised η of the resulting solution, a phenomenon observed in many

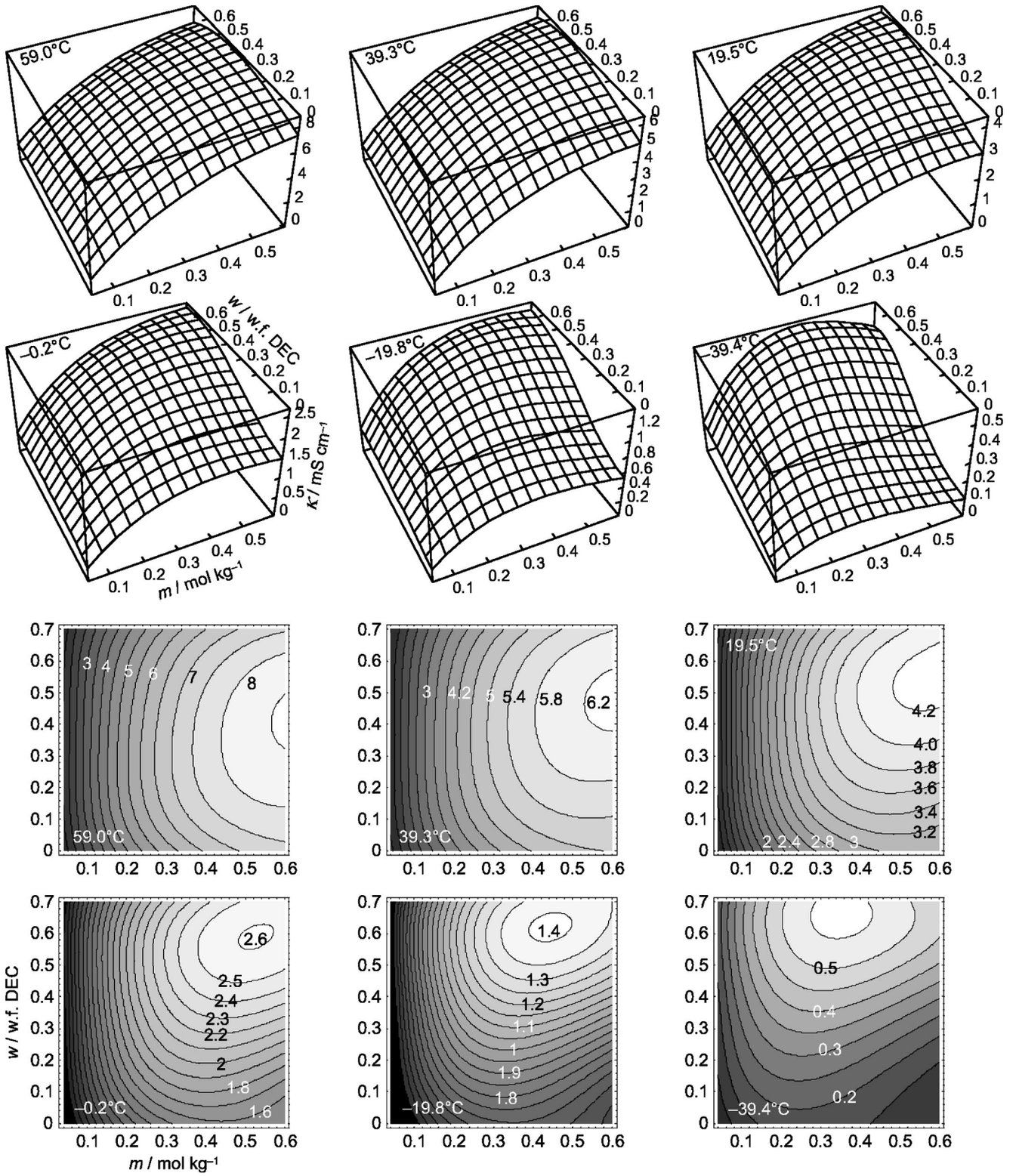

Figure 3. Change of conductivity κ with simultaneous changes in salt molality m and solvent weight fraction w for $(LiBOB)_m$-$PC_{1-w}DEC_w$ solution according to Eq. 2 that has been fitted to the measured $\kappa(m,w)$ data. Each function is doubly represented by a surface plot (upper plots) and a contour plot (lower plots) with the temperature and the contour values indicated in the plots.

Table I. Fitted values for the parameters of the fitting equation in the table for $(LiBOB)_m$-$PC_{1-w}DEC_w$ solution, with κ in the unit of $\mu S\ cm^{-1}$, application limits of 0.04 to 0.6 mol kg^{-1} for m and 0 to 0.7 weight fraction of DEC for w, and e_f as the fitting error as a percentage of the range of the fitting data.

$$\ln \kappa = \left(\sum_{i=0}^{4} a_i w^i\right) \ln m + \left(\sum_{i=0}^{4} b_i w^i\right) + \left(\sum_{i=0}^{4} c_i w^i\right) m + \left(\sum_{i=0}^{4} d_i w^i\right) m^2$$

θ/	a_0	a_1	a_2	a_3	a_4	b_0	b_1	b_2	b_3	b_4	c_0	c_1	c_2	c_3	c_4	d_0	d_1	d_2	d_3	d_4	e_f
59.0	0.96165	−0.5129	3.2595	-	5.5074	10.244	1.3119	−2.072	-	2.392	-	−0.36918	-	10.626	-	0.077921	-	9.0439	-	8.993	0.70
49.2	0.96465	-	3.6088	-	6.2615	10.11	1.2704	−1.0252	-	4.7822	-	−0.20697	-	18.11	−15.04	0.062622	-	12.775	-	17.944	0.68
39.3	0.96646	−0.575	3.8285	-	6.7696	9.9569	1.2392	-	-	6.6587	−1.598	0.040921	-	24.774	-	0.041859	-	16.857	-	26.876	0.67
29.4	0.96665	-	4.3301	-	7.7521	9.779	1.1406	1.4044	-	9.9238	-	0.47162	−10.3	36.008	-	0.005118	-	22.528	-	37.906	0.66
19.5	0.96717	-	4.9151	-	8.9583	9.5798	0.98018	3.2689	-	13.916	-	1.083	-	49.492	-	−0.03868	-	29.279	-	52.885	0.66
9.7	0.96792	-	5.4553	-	9.6587	9.3541	0.8478	4.9958	-	16.159	-	1.6318	−18.84	57.751	-	−0.0923	−4.964	35.337	-	59.784	0.66
−0.2	0.97055	-	6.5092	-	11.224	9.0923	0.5285	8.2743	-	21.143	-	2.7336	-	76.565	−61.37	−0.16623	-	45.488	-	74.309	0.67
-	0.9731	−1.0757	7.4987	-	12.57	8.7854	0.22825	11.334	-	25.306	-	3.8289	−33.73	91.059	−70.97	−0.2632	-	55.128	-	84.936	0.69
-	0.97875	−1.2197	8.301	−18.97	13.439	8.4265	0.006992	13.717	-	27.887	-	4.7783	-	99.613	-	−0.38868	-	63.833	-	91.657	0.72
-	0.9869	−1.2391	7.6684	−16.65	11.355	7.9979	0.30583	11.061	-	20.219	-	4.1605	-	63.148	-	−0.55901	−9.396	54.887	-	59.291	0.74
-	0.99907	−1.0749	5.7025	-	7.2373	7.4668	1.3996	3.4632	-	5.0935	-	1.2465	4.324	-	11.576	−0.80038	-	29.446	−26.665	-	0.70

other electrolytes.[1,6,9,13,22-24] It also appears that the rise of T_g due to the addition of salt was independent of that due to the change of solvent composition, which is most clearly seen in the absence of a cross-product term in the fitting function of Eq. 1. Although T_g of the $(LiBOB)_m$-$PC_{1-w}DEC_w$ solution could not be systematically measured due to the low solubility of LiBOB in PC-DEC, the limited data available showed a T_g rising with m and falling with w, as has been observed in the PC-DEC solutions of $LiPF_6$ and $LiBF_4$.[1,2]

Change of conductivity with salt content, solvent composition, and temperature

PC-DEC solution of LiBOB.—Results of the κ measurement from 60 to −40°C for $(LiBOB)_m$-$PC_{1-w}DEC_w$ and $(LiBOB)_m$-$PC_{1-w}EC_w$ solutions are plotted in Fig. 2 as 16 $\kappa(m)$ plots, one for each solvent composition. The open circles represent the measured data and the curves plot their fitting functions $\kappa(m,w)$ at the particular temperatures. These functions are extensions of the Casteel-Amis equation[1] by setting the equation parameters to polynomial functions of w.[1,2,5] That is

$$\kappa = m^a \exp(b + cm + dm^2) \qquad [2]$$

where a, b, c, and d are fourth degree polynomials of w for $(LiBOB)_m$-$PC_{1-w}DEC_w$

$$p = p_0 + p_1 w + p_2 w^2 + p_3 w^3 + p_4 w^4 \qquad [3]$$

and second degree polynomials of w for $(LiBOB)_m$-$PC_{1-w}EC_w$

$$p = p_0 + p_1 w + p_2 w^2 \qquad [4]$$

p in Eqs. 3 and 4 stands for a, b, c, or d. The choice of a higher degree for the polynomial of Eq. 3 was due to the relatively abrupt changes of κ with w in the PC-DEC solution of LiBOB. As shown in Fig. 2, the $\kappa(m,w)$ functions thus fitted are highly accurate in describing the measured $\kappa(m,w)$ data, as has been the case for other solutions.[1,2,5]

A more important use of those $\kappa(m,w)$ functions is to plot out the κ surfaces for the observation of change in κ with simultaneous changes of m and w. Such plots are shown in Fig. 3 for $(LiBOB)_m$-$PC_{1-w}DEC_w$ for θ from 60 to −40°C in a 20° interval, once as a surface plot and once as a contour plot for each. The functions used to generate these plots are given in Table I, with their parameter values listed in the same temperature range in a 10° interval. The most conspicuous feature emerging from these plots is the "dome" shape of the κ surfaces, as a result of κ peaking in both m and w. Peaking of κ in m is a common feature for liquid electrolytes, reflecting the process of κ first increasing with the number of dissociated ions as m increases and then falling as the rise in η and in ion association become dominant; this has been observed for many electrolytes of lithium salts.[1,2,5-7,14,15,22,31-33] Peaking of κ in w, on the other hand, seems to be the result of the ε and η of DEC both being much lower than those of PC and both being monotonic functions of w. As such, as w rises from zero, the change of κ is first dominated by the fall of η of the electrolyte causing κ to rise and then by the fall of ε of the solvent which by allowing stronger ion association causes κ to fall. The same behavior has been observed in $LiPF_6$-(PC-DEC),[1] $LiBF_4$-(PC-DEC),[2] and $LiPF_6$-(EC-EMC),[7] where the linear carbonates DEC and EMC have much lower ε and η than their cyclic counterparts PC and EC, and in $LiClO_4$-(PC-DME)[8] and $NaClO_4$-(PC-DME),[9] where DME (dimethoxyethane) has a much lower ε and η than PC.

PC-EC solution of LiBOB.—The $\kappa(m,w)$ fitting functions for $(LiBOB)_m$-$PC_{1-w}EC_w$ solution are plotted in Fig. 4 and listed in Table II. Compared to the results for $(LiBOB)_m$-$PC_{1-w}DEC_w$, the κ surfaces here assume the shape of an "arch" instead of a dome, κ

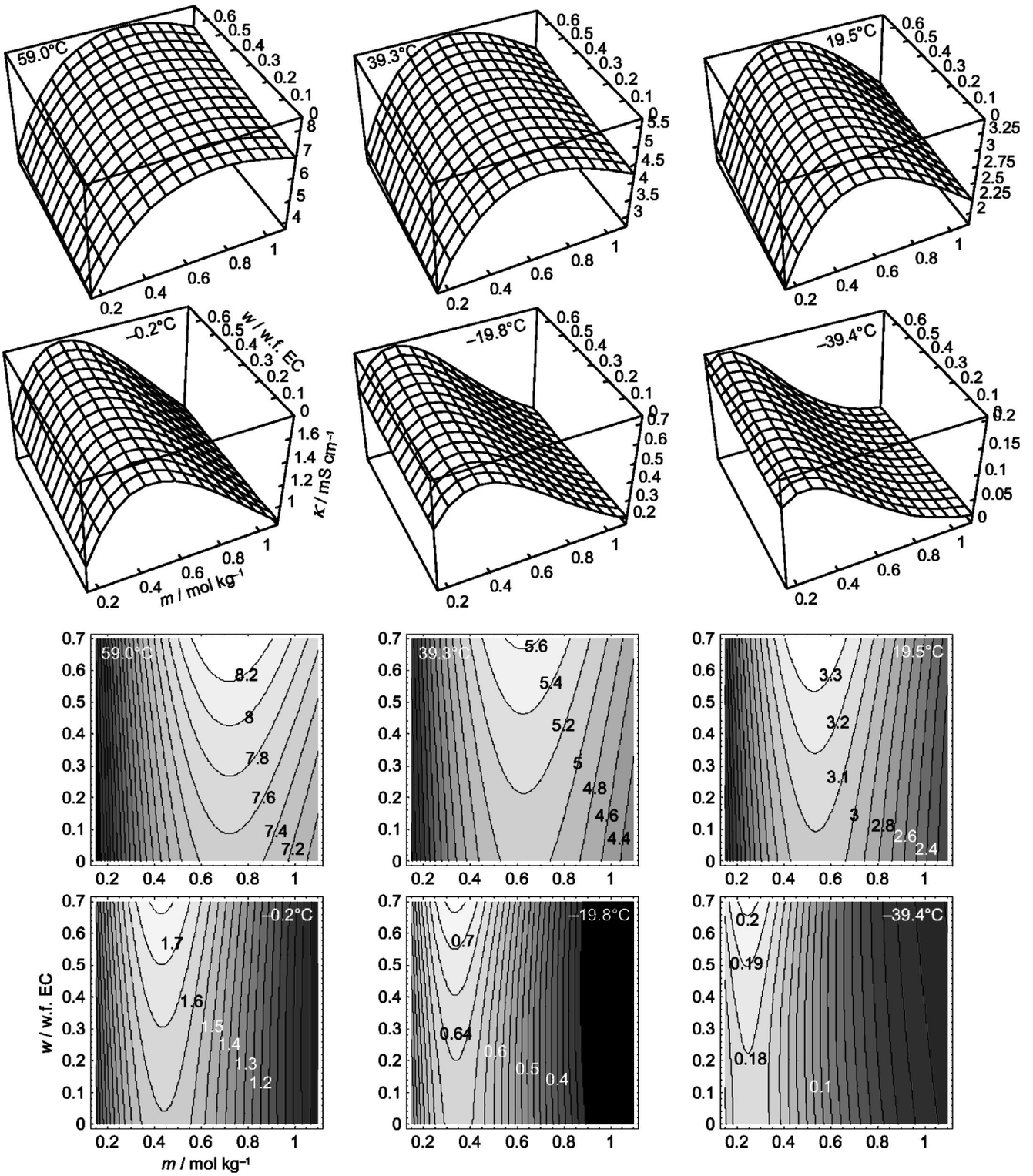

Figure 4. Change of conductivity κ with simultaneous changes in salt molality m and solvent weight fraction w for $(LiBOB)_m$-$PC_{1-w}EC_w$ solution according to Eq. 2 that has been fitted to the measured $\kappa(m,w)$ data. Each function is doubly represented by a surface plot (upper plots) and a contour plot (lower plots) with the temperature and the contour values indicated in the plots.

peaking only in m but rising continuously with w. This is because compared to PC, EC has a considerably higher ε but only a slightly higher η. Thus, as w increases, ε of the solvent rises but η of the electrolyte remains very much the same, resulting in the constant dominance of a weakening ion association that causes the continuous rise in κ. But apart from the arch-dome difference, other features in the κ surfaces of Fig. 4 can all find their counterparts in Fig. 3, with the same underlying mechanisms.

Table II. Fitted values for the parameters of the fitting equation in the table for $(LiBOB)_m$-$PC_{1-w}EC_w$ solution, with κ in the unit of μS cm^{-1}, application limits of 0.1 to 1.1 mol kg^{-1} for *m* and 0 to 0.7 weight fraction of DEC for *w*, and e_f as the fitting error as a percentage of the range of the fitting data.

$\ln \kappa = (a_0 + a_1 w + a_2 w^2)\ln m + (b_0 + b_1 w + b_2 w^2) + (c_0 + c_1 w + c_2 w^2)m + (d_0 + d_1 w + d_2 w^2)m^2$

θ/°C	a_0	a_1	a_2	b_0	b_1	b_2	c_0	c_1	c_2	d_0	d_1	d_2	e_f
59.0	0.88657	−0.02148	0.04276	10.11	0.057476	0.14648	−1.2514	0.12655	−0.14324	0.014022	−0.06228	0.047378	0.19
49.2	0.8897	−0.01865	0.034648	9.9749	0.068694	0.12572	−1.3091	0.099599	−0.10103	−0.00577	−0.06095	0.032203	0.17
39.3	0.88641	−0.01135	0.029487	9.8072	0.089044	0.11553	−1.348	0.055458	−0.07918	−0.04596	−0.04761	0.020391	0.18
29.4	0.88769	−0.03861	0.057642	9.6324	0.036699	0.17047	−1.4284	0.13761	−0.1601	−0.07644	−0.09922	0.055123	0.19
19.5	0.88715	−0.03482	0.046169	9.4294	0.0464	0.14977	−1.514	0.12685	−0.13213	−0.12308	−0.12575	0.057463	0.24
9.7	0.88933	−0.04056	0.0545	9.2064	0.036557	0.16769	−1.641	0.14522	−0.1587	−0.17096	−0.17173	0.077485	0.30
−0.2	0.88388	−0.02862	0.034264	8.9222	0.07647	0.1121	−1.7512	0.052539	−0.02622	−0.26911	−0.16786	0.015418	0.32
−10.0	0.87862	−0.02399	0.010599	8.5912	0.10444	0.042343	−1.8982	−0.1031	0.30454	−0.40046	−0.11387	−0.22237	0.28
−19.8	0.88497	−0.08009	0.036229	8.233	−0.04324	0.11782	−2.1809	0.1422	0.30346	−0.52423	−0.36719	−0.20569	0.26
−29.5	0.87839	0.013384	−0.15863	7.7628	0.13266	−0.17408	−2.4787	−0.18553	0.7611	−0.73899	−0.40724	−0.3349	0.30
−39.4	0.882	−0.06813	0.084147	7.2015	−0.01231	0.24496	−2.934	−0.29115	0.94329	−1.0204	−0.3694	−1.1727	0.30

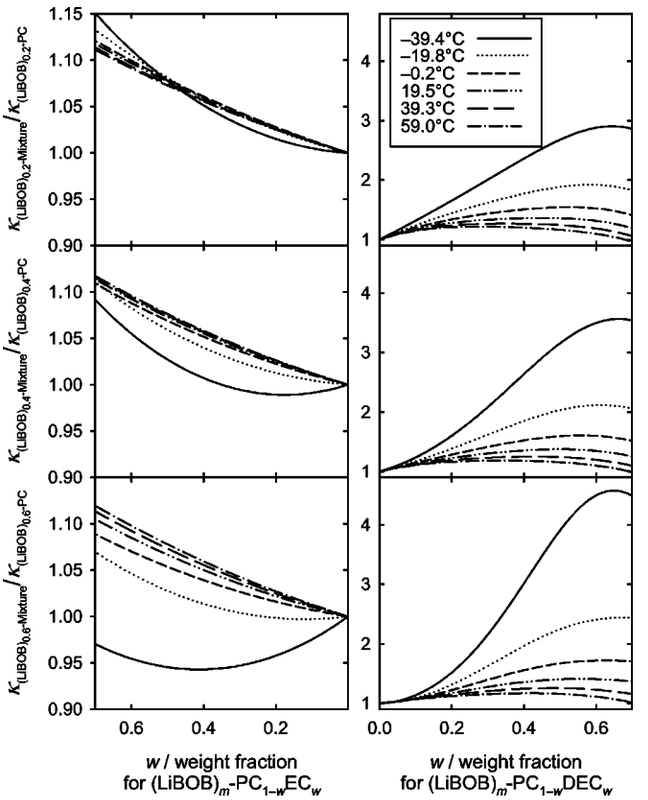

Figure 5. Change of conductivity κ with solvent weight fraction *w* of DEC and EC for $(LiBOB)_m$-$PC_{1-w}DEC_w$ and $(LiBOB)_m$-$PC_{1-w}EC_w$ solutions at different temperatures for three different salt molalities as indicated in the plots. The ordinate values of these plots are ratios of the conductivity of $(LiBOB)_m$-$PC_{1-w}DEC_w$ (right column) or of $(LiBOB)_m$-$PC_{1-w}EC_w$ (left column) over that of $(LiBOB)_m$-PC.

Comparison of the PC-DEC and PC-EC solutions.—To observe and compare the effects of the DEC and EC content on the κ of the two solutions more quantitatively, the ratios of κ of $(LiBOB)_m$-$PC_{1-w}DEC_w$ and of $(LiBOB)_m$-$PC_{1-w}EC_w$ over the κ of $(LiBOB)_m$-PC are plotted in Fig. 5. Comparison of the two columns of plots for the two solutions shows that the variation in κ with *w* is much greater for $(LiBOB)_m$-$PC_{1-w}DEC_w$ than for $(LiBOB)_m$-$PC_{1-w}EC_w$, as a result of PC having an η much higher than DEC but only slightly lower than EC as discussed previously. This also explains the need for a higher degree in the polynomial of Eq. 3 than that of Eq. 4. The great enhancement in κ by the DEC addition, especially under high-η situations accompanied by a low θ and high *m*, can be clearly seen in the right column for $(LiBOB)_m$-$PC_{1-w}DEC_w$. With increasing DEC content in the LiBOB-PC, the κ of the resulting solution invariably rises initially due to the reduction in η of the solution, though it eventually peaks and falls due to the excessive fall in ε of the solvent. Furthermore, the degree of the rise in κ increases with lower θ and higher *m* and can grow to be quite high; for instance, at −39.4°C, κ of $(LiBOB)_{0.6}$-$PC_{0.4}DEC_{0.6}$ more than quadruples that of $(LiBOB)_{0.6}$-PC. These observations clearly demonstrate the dominance of η in determining the κ of the LiBOB-PC-DEC solution.

The plots of the left column for $(LiBOB)_m$-$PC_{1-w}EC_w$ show a steady rise in κ with *w*, demonstrating the overwhelming dominance of change of ε with *w* over that of η due to the closeness in η between PC and EC. In addition, at lower *m*, the rise of κ with *w* speeds up slightly with lowering θ, in complete agreement with the result of a Bjerrum critical distance falling slowly with a lowering θ

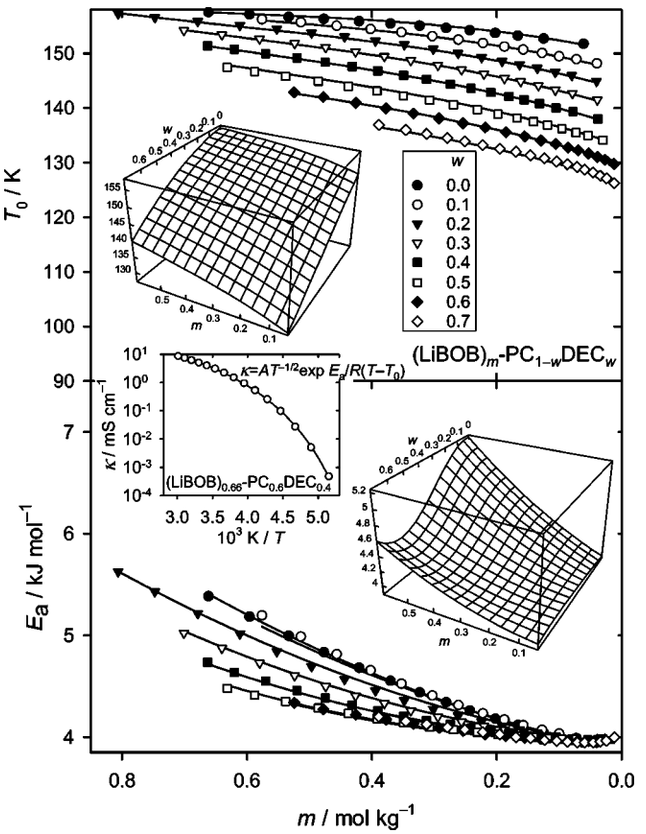

Figure 6. Results of fitting the measured $\kappa(T)$ data with the VFT equation of Eq. 5 for (LiBOB)$_m$-PC$_{1-w}$DEC$_w$ solution at different salt molalities m and solvent weight fractions w. The upper and the lower plots describe respectively the vanishing mobility temperature T_0 and the apparent activation energy E_a, with the open circles representing the results from fitting Eq. 5 and the curves and the surfaces representing the polynomial functions of Eqs. 6 and 7 obtained from fitting the data of the open circles.

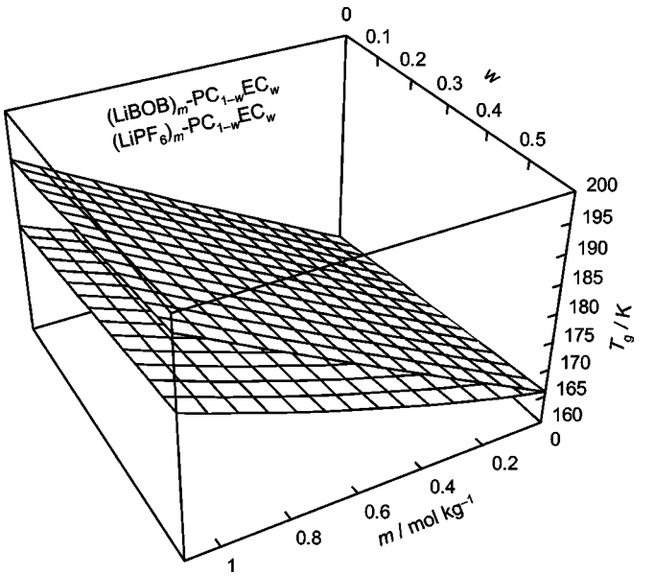

Figure 7. Comparison of T_g surfaces of (LiBOB)$_m$-PC$_{1-w}$EC$_w$ and (LiPF$_6$)$_m$-PC$_{1-w}$EC$_w$ solutions in the coordinates of salt molality m and solvent weight fraction w.

obtained in a previous study.[4] However, as m rises and θ falls, the κ eventually starts to decrease with w, as shown in the lower-left plot of Fig. 5, which is likely due to a higher η of the EC-solution than that of the PC-solution at these high values of m and low values of θ. In view of the very similar values of η between EC and PC around room temperature, one must conclude that the η of EC decreases with a lowering θ faster than that of PC, with or without the participation of the ions. Even at these situations where the rising η initially causes κ to decrease, the rising ε eventually dominates the rising η and causes κ to increase, thus forming minima in the $\kappa(w)$ curves as shown in the plots of the left column of Fig. 5.

Fitting κ-T data with VFT equation.—Measured $\kappa(T)$ data of an electrolyte, especially at temperatures close to its T_g, are often fitted with the Vogel-Fulcher-Tammann equation[34]

$$\kappa = \frac{A}{\sqrt{T}}\exp\left(-\frac{E_a}{R}\frac{1}{T-T_0}\right) \qquad [5]$$

resulting in an evaluation of the fitting parameters A, E_a (the apparent activation energy), and T_0 (the vanishing mobility temperature).[16,17,35,36] This was done for the (LiBOB)$_m$-PC$_{1-w}$DEC$_w$ solution on its $\kappa(T)$ data from 60 to −80°C, of which the results are shown in Fig. 6 for T_0 and E_a, with an average fitting error of 0.24% of the data range. An example of the fit for an electrolyte of (LiBOB)$_{0.66}$-PC$_{0.6}$DEC$_{0.4}$ is plotted as an insert in the figure. These fitting values as plotted with the open circles in Fig. 6 were further fitted with polynomial functions, which are also plotted in the figure with the curves and the 3D surfaces. These polynomials are, for T_0 and E_a in the upper and lower plots, respectively

$$T_0 = 150.21 + 24.842m - 32.489m^2 + 17.673m^3 - 33.919w + 44.607mw - 40.809mw^2 \qquad [6]$$

where the application limits are 0.04 to 0.6 mol kg^{-1} for m and 0 to 0.7 weight fraction for w and the fitting error is 0.78% of the data range, and

$$E_a = 3.85 + 1.3326m + 1.5421m^2 + 0.31334w - 14.636mw^2 + 17.532mw^3 - 0.77621w^5 \qquad [7]$$

where the application limits are the same as those of Eq. 6 and the fitting error is 1.4% of the data range. These equations represent relatively simple surfaces with a general downward slant from the high-η corner of high m and low w to the low-η corner of low m and high w, as shown by the 3D inserts in Fig. 6. This general association of a higher E_a with a higher η has been observed in other electrolyte systems, indicating in the electrolytes of this study a low degree of decoupling between the motion of ion and of solvent body or a high degree of assistance the solvent molecules provide to the ion transport.[1,2,16,17] For comparison, E_a has been evaluated to range from 3.7 to 5.8 kJ mol^{-1} for LiPF$_6$-(PC-DEC) solution,[1] from 3.2 to 5.6 kJ mol^{-1} for LiBF$_4$-(PC-DEC) solution,[2] from 4.2 to 4.8 kJ mol^{-1} for some low-η electrolytes,[13] and from 5.5 to 9.4 kJ mol^{-1} for some low-melting molten salts.[36]

The same treatment of $\kappa(T)$ data for (LiBOB)$_m$-PC$_{1-w}$EC$_w$ has led to a T_0 surface slanting down from the high-η corner (high m and w) to the low-η corner (low m and w). Compared to the T_g surface of Fig. 1, the T_0 surface has the same orientation and is lower in value by more than 10 K, a situation found in the PC-DEC solutions of LiPF$_6$ and LiBF$_4$ and in other electrolytes.[1,2,6,7,35,37]

Comparison of LiBOB with LiPF$_6$ *for their* T_g *and* κ.—To compare the effects of LiBOB and LiPF$_6$ on the η of the electrolytes, the

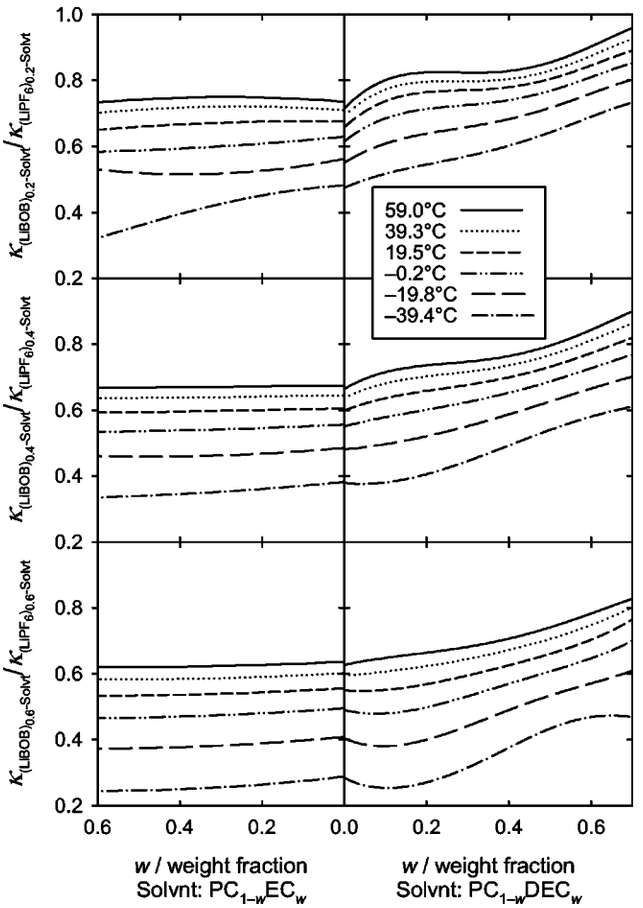

Figure 8. Change with solvent weight fraction w of the ratio of κ of $(LiBOB)_m$-$PC_{1-w}DEC_w$ over $(LiPF_6)_m$-$PC_{1-w}DEC_w$ (right column) and of $(LiBOB)_m$-$PC_{1-w}EC_w$ over $(LiPF_6)_m$-$PC_{1-w}EC_w$ (left column) at salt molalities 0.2 mol kg^{-1} (top row), 0.4 mol kg^{-1} (middle row), and 0.6 mol kg^{-1} (bottom row), each at six different temperatures as marked in the figure.

T_g surface of Fig. 1 is replotted in Fig. 7 together with that of $LiPF_6$ obtained from a previous study.[1] As shown, the T_g of LiBOB is consistently higher than that of $LiPF_6$, with the difference increasing with higher m and w. This indicates that although both salts raise the η of the electrolytes, the effect is considerably stronger for LiBOB than $LiPF_6$. This is most likely the result of a weaker ion association of BOB^- than PF_6^- with Li^+ in the electrolytes due to the larger size of BOB^-, which leaves more free Li^+ to bind to the solvating solvent molecules and to thereby make the electrolyte more viscous. By this mechanism, the disparity in η between the two salts would increase with m and w, as is shown in Fig. 7.

The higher η of LiBOB than $LiPF_6$ also explains the differences in κ of the two salts in the same solvents, as shown in Fig. 8 where the ratio in κ of LiBOB in PC-DEC and PC-EC over $LiPF_6$ in the same solvents is plotted as a function of solvent composition at six temperatures and three salt concentrations. As can be seen, this ratio is below unity for all situations, mainly as a result of the higher η of LiBOB than $LiPF_6$ solution. It also becomes substantially lower with lower θ, as can be seen in each of the frames. It does the same, though not quite as dramatically, with higher m, as seen from the top to the bottom row, and with the richer content of the more viscous component of the solvent, as seen from the right to the left column. In short, the ratio is lower whenever the η of the electrolyte is higher, manifesting the total dominance of η over ion association in determining the relative κ values of the two electrolyte systems.

Conclusions

Glass transition temperature T_g of PC-EC solution of LiBOB rose with salt molality m and weight fraction w of EC, the effects of m and w being largely independent of each other. Conductivity κ of the PC-DEC solution of LiBOB, in its change with m and w at different temperatures θ, peaked in both variables and thus formed a ''dome'' when plotted as a 3D surface in the mw-coordinates, while κ of the PC-EC solution of LiBOB peaked only in m thus assuming an ''arch''-shaped surface. This dome-arch difference was primarily due to PC having a dielectric constant ε much higher than DEC but considerably lower than EC, and a viscosity η much higher than DEC but only slightly lower than EC. In addition, as θ was lowered, the κ surfaces fell in height and shifted in position in the direction of low η. All these observations were the results of the interplay of ε of the solvents and η of the electrolytes at different values of m, w, and θ. The effects of DEC and EC on the κ of PC solution of LiBOB demonstrated the dominance of η in determining κ and the weak dependence of ion association on θ. Fitting VFT equation to the measured $\kappa(T)$ data of the PC-DEC solution of LiBOB resulted in an evaluation of its vanishing mobility temperature T_0 and apparent activation energy E_a, both forming simple surfaces in the mw-coordinates slanting up in the direction of high η. Furthermore, relative to the T_g and κ of $LiPF_6$ in the same solvents, the T_g of LiBOB was consistently higher, with the difference becoming greater at higher m and richer content in the more viscous component of the solvent, and the κ of LiBOB grew lower in electrolytes of higher η.

Acknowledgment

We thank the U.S. Department of Energy, Office of FreedomCar and Vehicle Technologies for partial funding of this work.

The Army Research Laboratory assisted in meeting the publication costs of this article.

References

1. M. S. Ding and T. R. Jow, *J. Electrochem. Soc.*, **150**, A620 (2003).
2. M. S. Ding, *J. Electrochem. Soc.*, **151**, A40 (2004).
3. I. Mills, T. Cvitas, K. Homann, N. Kallay, and K. Kuchitsu, *Quantities, Unites and Symbols in Physical Chemistry*, 2nd ed., p. 48, IUPAC and Blackwell Scientific Publications, London (1993).
4. M. S. Ding, *J. Electrochem. Soc.*, **150**, A455 (2003).
5. M. S. Ding, *J. Chem. Eng. Data*, **48**, 519 (2003).
6. M. S. Ding, K. Xu, and T. R. Jow, *J. Electrochem. Soc.*, **149**, A1489 (2002).
7. M. S. Ding, K. Xu, S.-S. Zhang, K. Amine, G. L. Henriksen, and T. R. Jow, *J. Electrochem. Soc.*, **148**, A1196 (2001).
8. Y. Matsuda, M. Morita, and K. Kosaka, *J. Electrochem. Soc.*, **130**, 101 (1983).
9. Y. Matsuda and H. Satake, *J. Electrochem. Soc.*, **127**, 877 (1980).
10. *Electrolyte Data Collection, Part 2a, Dielectric Properties of Nonaqeous Electrolyte Solutions*, Vol. XII, J. Barthel, R. Buchner, and M. Munsterer, Editors, Chemistry Data Series, DECHEMA, Frankfurt (1996).
11. *Electrolyte Data Collection, Parts 3a and 3b, Viscosity of Non-Aqeous Solutions II: Aprotic and Protic Non-Alcohol Solutions C1-C3 and C4-C8*, Vol. XII, J. Barthel, R. Neueder, and R. Meier, Editors, Chemistry Data Series, DECHEMA, Frankfurt (2000).
12. *Electrolyte Data Collection, Part 1d, Conductivities, Transference Numbers and Limiting Ionic Conductivities of Aprotic, Protophobic Solvents II. Carbonates*, Vol. XII, J. Barthel and R. Neueder, Editors, Chemistry Data Series, DECHEMA, Frankfurt (2000).
13. Y. Matsuda, M. Morita, and T. Yamashita, *J. Electrochem. Soc.*, **131**, 2821 (1984).
14. J. Barthel, R. Buestrich, E. Carl, and H. J. Gores, *J. Electrochem. Soc.*, **143**, 3565 (1996).
15. H. P. Chen, J. W. Fergus, and B. Z. Jang, *J. Electrochem. Soc.*, **147**, 399 (2000).
16. G. Y. Gu, S. Bouvier, C. Wu, R. Laura, M. Rzeznik, and K. M. Abraham, *Electrochim. Acta*, **45**, 3127 (2000).
17. G. Y. Gu, R. Laura, and K. M. Abraham, *Electrochem. Solid-State Lett.*, **2**, 486 (1999).
18. *Handbook of Organic Solvents*, D. R. Lide, Editor, CRC Press, Boca Raton, FL (1995).
19. G. E. Blomgren, in *Lithium Batteries*, J.-P. Gabano, Editor, Academic Press, London (1983).
20. J. Barthel, R. Neueder, and H. Roch, *J. Chem. Eng. Data*, **45**, 1007 (2000).

21. R. Payne and I. E. Theodorou, *J. Phys. Chem.*, **76**, 2892 (1972).
22. A. Cisak and L. Werblan, *High-Energy Non-aqueous Batteries*, Ellis Horwood, New York (1993).
23. J. F. Casteel, J. R. Angel, H. B. McNeeley, and P. G. Sears, *J. Electrochem. Soc.*, **122**, 319 (1975).
24. G. Petrella and A. Sacco, *J. Chem. Soc., Faraday Trans. 1*, **74**, 2070 (1978).
25. G. M. Ehrlich, in *Handbook of Batteries*, 3rd ed., D. Linden and T. B. Reddy, Editors, McGraw-Hill, New York (2002).
26. S. Hossain, in *Handbook of Batteries*, 2nd ed., D. Linden, Editor, McGraw-Hill, New York (1995).
27. T. R. Jow, M. S. Ding, K. Xu, S. S. Zhang, J. L. Allen, K. Amine, and G. L. Henriksen, *J. Power Sources*, **119**, 343 (2003).
28. M. S. Ding, K. Xu, and T. R. Jow, *J. Electrochem. Soc.*, **147**, 1688 (2000).
29. U. Lischka, U. Wietelmann, and M. Wegner, Ger. Pat. DE 19829030 C1 (1999).
30. K. Xu, S.-S. Zhang, B. A. Poese, and T. R. Jow, *Electrochem. Solid-State Lett.*, **5**, A259 (2002).
31. J. F. Casteel and E. S. Amis, *J. Chem. Eng. Data*, **17**, 55 (1972).
32. J. Barthel, H. J. Gores, and G. Schmeer, *Ber. Bunsenges. Phys. Chem.*, **83**, 911 (1979).
33. Y. Choquette, G. Brisard, M. Parent, D. Brouillette, G. Perron, J. E. Desnoyers, M. Armand, D. Gravel, and N. Slougui, *J. Electrochem. Soc.*, **145**, 3500 (1998).
34. S. I. Smedley, *The Interpretation of Ionic Conductivity in Liquids*, Plenum Press, New York (1980).
35. J. Barthel, R. Meier, and B. E. Conway, *J. Chem. Eng. Data*, **44**, 155 (1999).
36. A. B. McEwen, H. L. Ngo, K. LeCompte, and J. L. Goldman, *J. Electrochem. Soc.*, **146**, 1687 (1999).
37. C. A. Angell and D. L. Smith, *J. Phys. Chem.*, **86**, 3845 (1982).